Low cutoff wavelength etched SMS structures towards verification of the quality of automotive antifreeze.

Wenceslao Eduardo Rodríguez-Rodríguez, Adolfo Josué Rodríguez-Rodríguez, Carlos R. Zamarreño, Ignacio Del Villar, Manuel Zúñiga-Alanís.

***Abstract*—Optical fiber single mode – multimode – single mode (SMS) structures can be used as wavelength detection-based sensors. In this work, we focus on the performance at short wavelengths, where optical sources and detectors are less expensive. Here, a self-image band with a high transmission power is monitored in this short-wavelength range. In addition, the diameter and the length of the SMS structure have been optimized in order to improve the sensitivity of the device. In this sense, a maximum refractive index sensitivity of 305 nm/RIU was achieved by an etched SMS with a diameter of 34 µm. Furthermore, the obtained devices were used for testing the quality of automotive coolant and antifreeze liquid.**

***Index Terms*—optical fiber, multimodal interference, self-image, etching, coolant, antifreeze.**

I. INTRODUCTION

Optical fiber sensors can be used in many applications due their interesting properties: small size, multiplexing capability and immunity to electromagnetic interferences [1-7]. Different fiber optic configurations have been studied for these purposes, such as those based on gratings (fiber Bragg gratings, long period gratings and tilted fiber Bragg gratings) or interferometers (Mach-Zender, Fabry-Pérot and Michelson) [1].

This manuscript was submitted on mm/ dd/ 2019. We appreciate the support from the Programa de Fortalecimiento de la Calidad Educativa (PFCE) and the Programa para el Desarrollo Profesional Docente (PRODEP), as well as by the Direction of strategic programs and projects of the Autonomus University of Tamaulipas (UAT) and the Direction of the Unit Academic Multidisciplinary Reynosa-Rodhe. To José Andrés Suárez Fernandez, Rector of the UAT for all the efforts made to obtain resources and continue supporting the research. Also, we appreciate the support from the Spanish Agencia Estatal de Investigación (AEI) and Fondo Europeo de Desarrollo Regional (FEDER) (TEC2016-78047-R), as well as by the Government of Navarra PC095-096 OPTISENS, PC081-082 BIOPTSENS AVANZA and Public University of Navarra PJUPNA26 research grants.

One of the simplest interferometric structures is the single mode – multi mode – single mode fiber (SMS), is based on the multimodal interference (MMI) effect [2]. Interferometers based on the SMS structures allow to observe wavelength shifts as a function of the surrounding medium's refractive index. However, most of the literature referencing these structures focus on its performance at telecommunications wavelengths (1100 to 1700 nm), requiring the utilization of expensive and complex experimental setups [3-7]. The performance of SMS structures at a shorter wavelength range (400-1000nm), permits the use of less expensive optical light sources and detectors [8,9]. However, the sensitivity at shorter wavelength range is reduced, hence it requires further optimization of these devices in order to overcome this limitation.

The sensitivity improvement has been previously attained reducing the structure diameter by means of an etching process through immersing of the device in hydrofluoric acid (HF). Concerning SMS structures, the diameter reduction was initially applied in devices operating at telecommunications wavelengths [3,4,6]. Recently, the idea was also explored with low cutoff wavelength SMS structures [8,9] for operation at shorter wavelengths.

Wenceslao Eduardo Rodríguez-Rodríguez, Adolfo Josué Rodríguez-Rodríguez and Manuel Zúñiga-Alanís are with the Computational Sciences and Technologies Department of the Autonomous University of Tamaulipas, CO 88690, Tamaulipas, Mexico (e-mails: wrodriguez@uat.edu.mx, arodriguez@uat.edu.mx, mazuniga@uat.edu.mx).

Carlos R. Zamarreño and Ignacio Del Villar are with Electrical, Electronic and Communication Engineering Department of the Public University of Navarra, CO 31006, Navarra, Spain (e-mails: carlos.ruiz@navarra.es, ignacio.delvillar@unavarra.es).

However, these works doesn´t pay attention to the self-image band, which is associated to the length of the device. In the present work, contrary to previous publications, a special focus is given to on the self-image band, where the optical transmission is maximum, as well as to the diameter and the length of the devices in order to position the transmission band in the wavelength range that is being monitored in the experimental setup. Different structures will be analyzed as a function of the refractive index for a better understanding of the basic rules that govern the position of the self-image band in the optical spectrum. Finally, the performance of the obtained structures is demonstrated in a practical application (the SMS structures has been previously used for detecting pH [9], glucose [10], quality of fuels [11] etc.). In this work, the SMS devices are used for testing the quality in coolants and antifreeze liquid of motor vehicles based on gasoline, which are very important in the automotive industry.

II. THEORETICAL BACKGROUND OF SMS STRUCTURES.

A. Principle of operation.

The SMS structure explored in this work consists of splicing a multimode "coreless" fiber (MMF-NC) segment to two single mode fiber (SMF) pigtails. In SMS structures, light transmitted through the core mode of the SMF is coupled to different propagation modes in the coreless segment, where light is in direct contact with the surrounding medium. This is the reason why SMS devices are sensitive to the external medium. In addition, due to the transmission of light in the coreless segment by modes with different effective index, the phase of the modes in the coreless segment is different at the point where light is coupled to the core mode of the output SMF segment, which causes constructive and destructive interference as a function of wavelength. In the coreless segment it is possible to find partial images at specific distances from the splice between the SMF and the MMF-NC segment [3] and [6]. This phenomenon is called multimodal interference effect [12]. The equation that rules the lengths where these images are created is expressed as

$$L = \rho\left[\left(n_{NC}\, {D_{NC}}^2\right)/\lambda\right] \tag{1}$$

where ρ is the order of the self-image, n_{NC} is the effective RI, D_{NC} is the waveguide diameter of MMF-NC and λ is the vacuum's wavelength. Several researches have focused particularly in the fourth self-image, because it is proved that at this specific order a narrow band-pass filter response is obtained [13]. A necessary condition to implement the SMS devices as refractometric sensors is that, the refractive index of surrounding medium must be lower than the MMF-NC [3,7].

B. Analysis to the sensitivity enhancement.

The fiber optic sensors based on the SMS configuration accomplish their operation due the absorption of the light carried by the evanescent wave in the sensible region of the structure, which allows the interaction with a surrounding refractive index (SRI), see Fig. 1. The evanescent wave is the optical wave that decays exponentially in the perpendicular direction to the MMF-NC/SRI interface. A remarkable parameter to take into account in the sensing purposes is the penetration depth D_p of the evanescent wave, this is the distance from the interface where the amplitude of the electric field decreases by a factor 1⁄e [14], expressed as

$$D_p = \frac{\lambda}{2\pi n_{NC}\sqrt{\sin^2\theta_i - \left(\frac{n_{SRI}}{n_{NC}}\right)^2}} \tag{2}$$

θ_i is the incident angle in the interface and n_{SRI} is the refractive index of the surrounding medium. Therefore, exists a ratio between D_p and SRI. In order to enhance the sensibility of the SMS structures it is necessary to increase the intensity of the evanescent wave by the increase of D_p, this can be achieved reducing the diameter in the sensitive region [15]. The application of corrosive materials makes possible to reduce the section of MMF-NC (typically HF is used). The lower the diameter is in the sensible region, higher will be the interaction between the interfered high-order modes and the SRI, producing a higher sensitivity in SMS structures [16].

In addition to the diameter reduction there are other aspects necessary to enhance the sensitivity in the SMS sensors. As higher the core's diameter is in SMF, longer will be the wavelength operation range of the SMS. This is important to consider, because when a self-image is established at longer positions the sensitivity is improved [8], because the penetration depth increases with the wavelength [17].

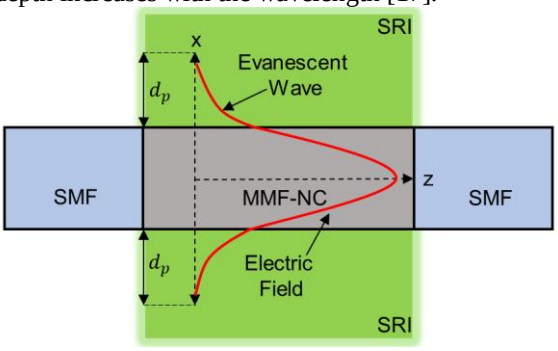

Fig. 1. Description of the evanescent wave in SMS devices.

C. Temperature influence in sensitivity.

The optical spectrum of the SMS structures depends on the temperature in the SRI due the inherent relationship with thermo-optic effects in the MMF-NC material, which allows a variation of its RI, causing a shift in the wavelength peak $\Delta\lambda$. This has been exposed by Aguilar-Soto *et al.* [7], the authors have demonstrated by testing the SMS structures in a hot environment (in air) the presence of sensitivity due of the increment of temperature. Besides, in S. Silva *et al.* [16], the authors have reported the presence of temperature sensivity in the spectral response in SMS devices when are exposed to a surrounding media (liquid) with RI=1.44 from 20°C to 80°C. The spectral response allows to observe that, when the temperature increases the RI of the liquid and the sensitivity decreases.

III. MATERIALS AND METHODS

A. Experimental setup.

The SMS structures used consisted of MMF-NC (FG125LA, *Thorlabs*), spliced to two SMF S630-HP pigtails (core diameter 3.5 μm and cladding diameter 125 μm, NA = 0.12 and operating wavelength 630– 860 nm). The devices were spliced and fused by A9 Tumtec and V9 Mini ICOptiks. The structures were fixed to a U-Holder (glass) to keep the sensitive region straight during the process of etching and interrogation of automotive liquids. In addition, an HL-2000 white light source and an USB4000 VIS-NIR spectrometer, both from Ocean Optics. The etching was performed inside a closed plastic container, the MMF- NC segment was inserted into a PLA cuvette where the HF was deposited, see Figure 2. In order to manipulate the devices in the interrogation process, an XZ robot was required. The devices were immersed in the samples, consecutively washed with distilled water and dried in air. All the liquids were placed into PLA containers, while the robot was controlled by LabVIEW (see Figure 3).

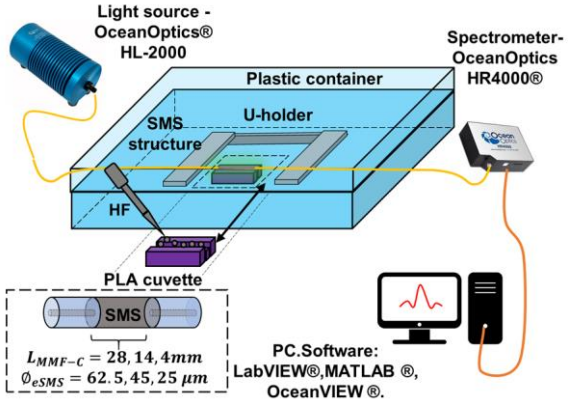

Fig. 2. Experimental setup applied for monitoring the optical spectrum during the etching process.

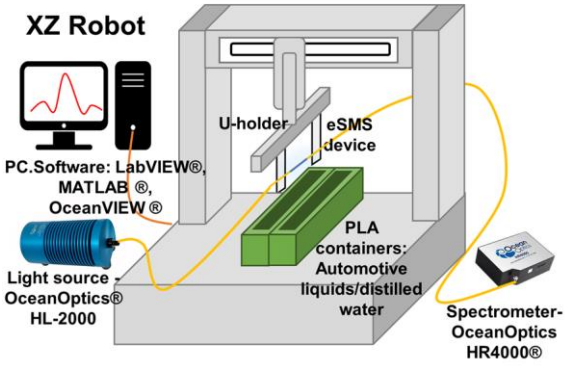

Fig. 3. Experimental setup used to monitoring the optical spectrum during the interrogation process for testing the quality of coolants and antifreeze liquids.

B. Diameter reduction.

Three SMS devices were fabricated: eSMS1, eSMS2 and eSMS3; with different lengths of *coreless* fiber: $L_{eSMS1} \approx 26mm$, $L_{eSMS2} \approx 13mm$ and $L_{eSMS3} \approx 7mm$. The length of MMF-C segment was measured by a millimeter ruler. These lengths were obtained by the use of eq. (1) for a reference wavelength peak at $\sim 800\ nm$, $\rho = 4$, $n = 1.4525$ and the specifics diameters ($D_{MMF} = \emptyset_{eSMS}$) in the sensitive region ($\emptyset_{eSMS1} \approx 60\ \mu m, \emptyset_{eSMS2} \approx 45\ \mu m$ and $\emptyset_{eSMS3} \approx 31\ \mu m$). Each structure was etched with HF at 48% during: eSMS1=25 minutes, eSMS2=30minutes and eSMS3=35minutes respectively. The fibers were rinsed in water afterwards in order to remove the HF excess after the etching process. Finally, the structures were left in air for at least 4 hours.

C. Automotive coolant and antifreeze.

Quality in automotive antifreeze is very important according to the regulations established by the governments and automotive industry [18-20]. The main purpose of the antifreeze liquid is to control the temperature of fluids and parts in the engine of a car; absorbing the heat from the engine to be then taken out by the radiator. In addition, the automotive industry refers with different names the two mixtures of antifreeze: coolant when the fabrication is based on distilled water/ethylene glycol concentrations of 50/50, 60/40, 70/30 and antifreeze when it is just based on ethylene glycol at 95% (5% additives). The composition of coolants and antifreezes have an optical relationship due their refractive indices. Based on the mentioned percentages of concentration and by the following equation is possible to calculate RI in coolants

$$n = [n_1 v_1 + n_2 v_2] \quad (2)$$

where n_1 and n_2 are the refractive index, v_1 and v_2 are the volume respectively of the two compounds of the mixture. By the previous equation and considering the refractive index in water= 1.3290 and ethylene glycol= 1.4263 both at 800 nm[21]. So, the estimated refractive indices in coolants are: 50/50=1.3777, 60/40=1.3679, 70/30=1.3582; whereas in antifreeze at 95% of ethylene glycol= 1.4214. These results were obtained considering v_1 and v_2 defined by normalized volumes (from 0 to 1).

The use of ethylene glycol allows a higher boiling point in the antifreeze liquids and a higher engine operating temperature in the coolants. Additionally, the freezing point is also decreased. Therefore, the coolants are used in driving conditions at high temperature (dry or desert), whereas the antifreeze liquid is used in low temperature driving conditions (snow and ice). The chosen samples of coolant and antifreeze liquid were acquired from generic brands (coolants 1, 2, 3 and antifreeze 1, 2) and from recognized worldwide brands (coolants 4, 5 and antifreeze 3, 4). The manufacturers provide in the specification charts the percentage concentration of distilled water and ethylene glycol only in the coolant liquids 3, 4, 5 (25%, 33% and 33%) and the antifreeze samples 4, 5 (95% and 98%).

IV. EXPERIMENTAL RESULTS

A. Effect of diameter reduction.

In order to understand the effect of diameter reduction, a SMS structure of length 26 mm was subjected to an etching process. According to eq. (1) the first order self-image should be located initially at approximately 810 nm, something that agrees well with the transmission spectrum of Figs. 4 a) and b). During the etching process the bands shift progressively to shorter wavelengths, something that again agrees with expression (1), where the wavelength is proportional to the diameter. After 11 minutes of etching the 2nd self-image band is present, then the third one (22 minutes) and the fourth one (28 minutes). As the etching process happens the intensity of the optical response in SMS devices will be higher due to the changes in the reflection coefficient at the MMF-NC/SRI interface [16]. The etching process is continued until the optical fiber is destroyed. Here, it is interesting to remark that the wavelength shift rate of the bands increases during the etching process because the sensitivity of the device increases with the diameter reduction, something that has been also observed in [22].These experimental results can be verified by the contributions exposed by [13,16], where unlike for the rest of self-images, for the 2nd self-image an optical power decrease is observed. Therefore, this was the criterion followed to identify these self-images. Finally, the 4th self-image appears in the desired position as a wavelength peak with a highest amplitude in comparison with the previous self-images. The duration of the etching process is dependent of parameters such as: percentage concentration of HF and temperature. When the values of both parameters increase, minor will be the time of the process [15, 16].

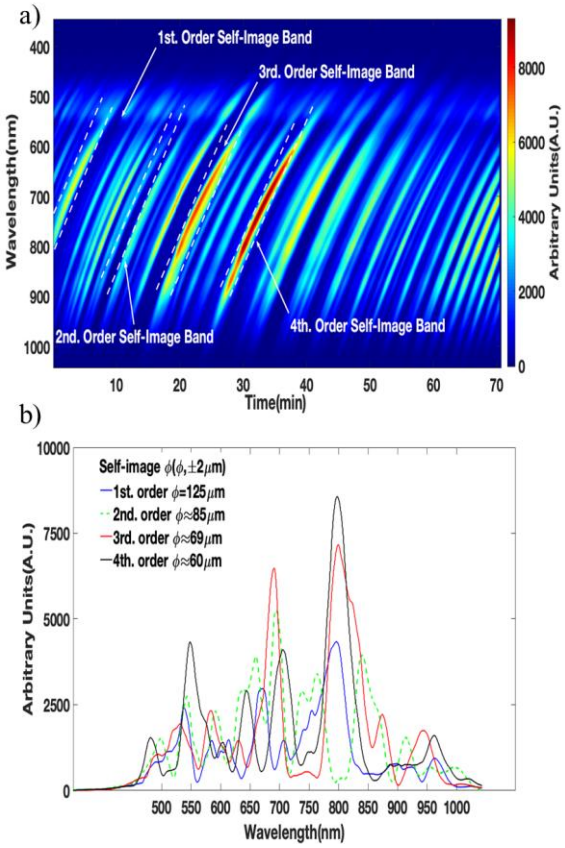

Fig. 4. SMS structure with coreless segment length 26 *mm* etched down to breakage of the device: a) Evolution of the transmission spectrum as a function of time; b) Transmission spectra corresponding first to fourth order self-images in the SMS structure.

B. Tuning of the 4th self-image band.

This subsection presents the fabrication process of the eSMS1, eSMS2 and eSMS3 structures. The following experiments have been verified according the eq. (1) at 800 nm.The fabrication of eSMS1 was developed following the same method described in Section IV. A. Due slight variations in the refractive index and diameter of the MMF-NC the first self-image appears at 850 nm, this fact is corroborated by [11]. The first self-image at 800 nm, occurs when the eSMS possesses a diameter $\approx 120.5\ \mu m$ (2 minutes after beginning the etching). The process has finished after 25 minutes of corrosion, when the 4th order self-image band appears. The transmission spectra of

eSMS1 during the etching process are shown in Figs. 5 a) and b).

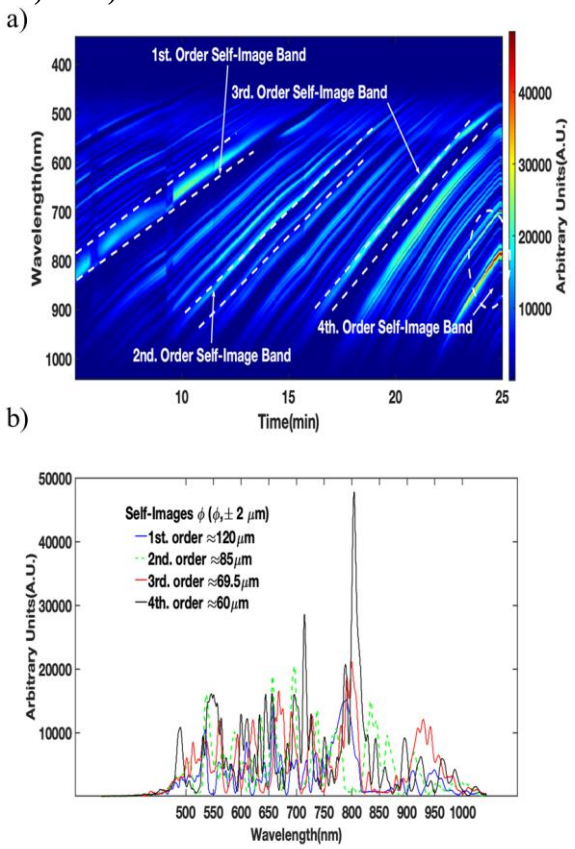

Fig. 5. eSMS1 structure with coreless segment length 26 mm etched down to a diameter of 60 µm: a) Evolution of the transmission spectrum as a function of time; b) Transmission spectra corresponding first to fourth order self-images in the SMS structure.

In eSMS2, the first order self-image band at a diameter $\approx 85\,\mu m$, occurs after 5 minutes of the etching. The whole fabrication process of eSMS2 is depicted in the Fig 6 a) and b). After that, there is a period without spectral replicas (12 minutes, $\emptyset \approx 60\,\mu m$), which is considered the 2nd order self-image band. Then, we can observe the presence of a spectral transmission band that possesses a wavelength peak with high amplitude, it is the 3rd order self-image band (23 minutes, $\emptyset \approx 49\,\mu m$). Finally, the wavelength peak appears with the narrowest bandwidth, being this the fourth order self-image band (29 minutes, $\emptyset \approx 45\,\mu m$)

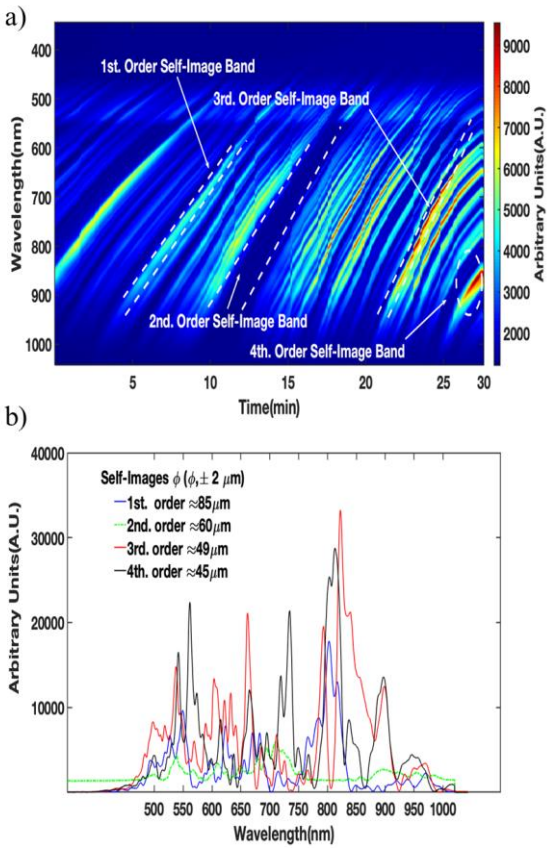

Fig. 6. eSMS2 structure with coreless segment length 13 mm etched down to a diameter of 45 µm: a) Evolution of the transmission spectrum as a function of time; b) Transmission spectra corresponding first to fourth order self-images in the SMS structure.

The eSMS3 device was fabricated following the same methodology in the etching process, see Fig. 7 a) and b). In order to corroborate the diameter obtained by etching in the fabricated eSMS structures, it was necessary to use a digital microscope AmScope b120 and the software IC Measure. The diameters in the devices were: eSMS1≈ 63.35μm, eSMS2≈ 42.11μm, eSMS3≈ 34.4 μm, presented in Fig. 8.

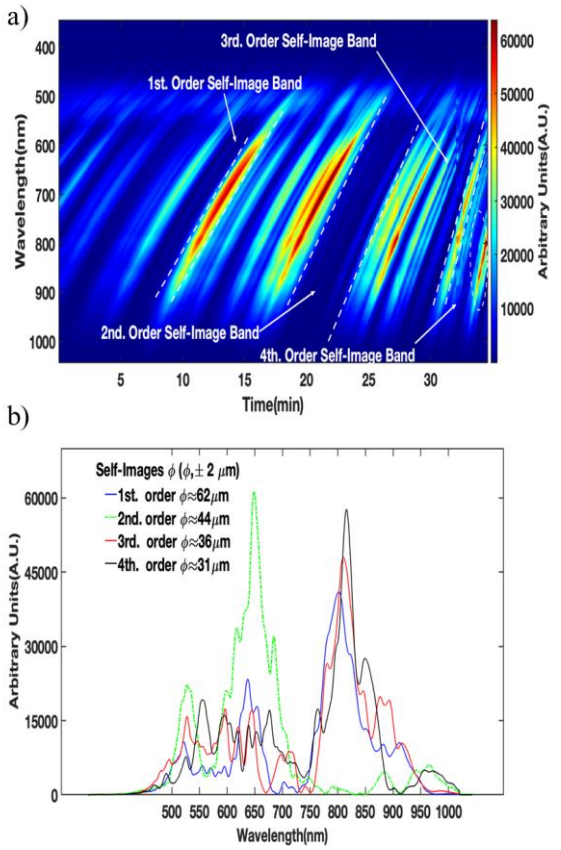

Fig. 7. eSMS3 structure with coreless segment length 7 mm etched down to a diameter of 31 µm: a) Evolution of the transmission spectrum as a function of time; b) Transmission spectra corresponding first to fourth order self-images in the SMS structure.

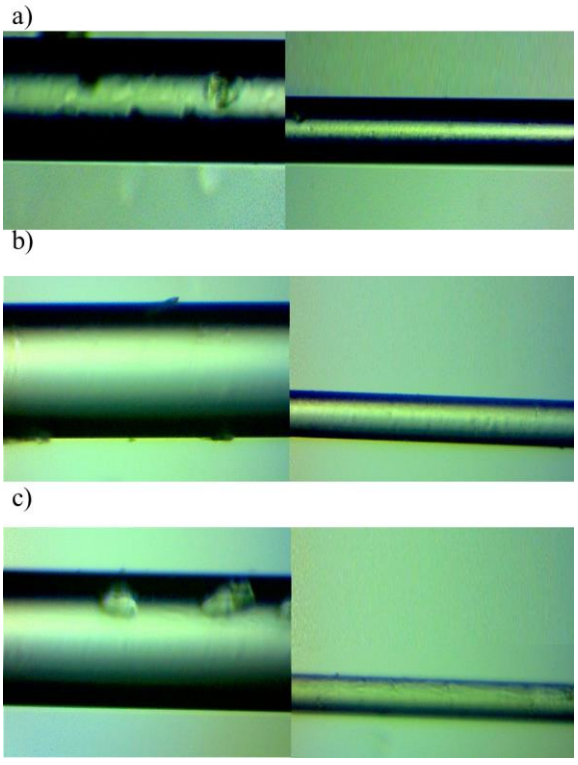

Fig. 8. Original diameter in SMS = 125 μm in comparison with the devices fabricated: a) eSMS1≈ 63.35μm. b) eSMS2≈ 42.11μm. c) eSMS3≈ 34.4 μm.

.

C. Application: Quality test of automotive coolants and antifreeze.

Previously to present the results obtained with automotive liquids, the devices have been tested in water, ethanol and ethylene glycol, which allow to characterize their relative wavelength shifts at three known refractive indices: water=1.3281, ethanol=1.3575 and ethylene glycol=1.4263, at 800 nm. The results are exposed in Fig. 9. The eSMS1 shows a wavelength shift $\Delta_{\lambda_{eSMS1}}\approx$ 11.308 nm and a sensitivity ≈ 115.23 nm/RIU, the eSMS2 shows a $\Delta_{\lambda_{eSMS2}}\approx$ 20.17 nm and a RI sensitivity ≈ 205.60 nm/RIU, whereas eSMS3 shows a $\Delta_{\lambda_{eSMS1}}\approx$ 24.08nm and a RI sensitivity ≈ 245.46 nm/RIU. Fig. 10, is illustrated the simulated behavior of the eSMS devices in refractive index from 1.33 to 1.43 (provided by FIMMWAVE).

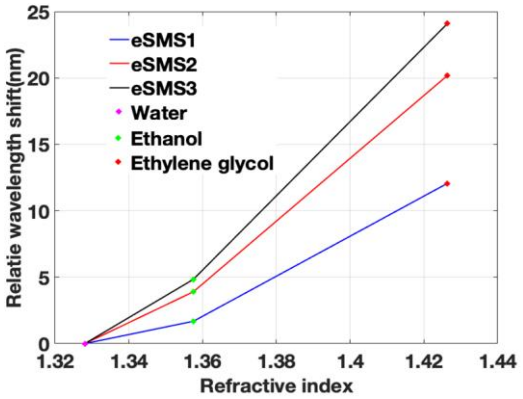

Fig. 9. Relative wavelength shifts of the devices: eSMS1, eSMS2 and eSMS3 for water, ethanol and ethylene glycol.

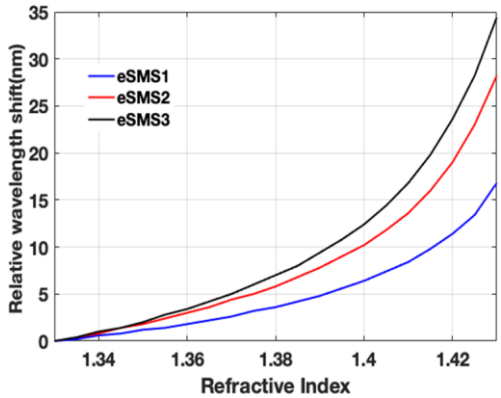

Fig. 10. Simulation of the relative wavelength shifts in: eSMS1, eSMS2 and eSMS3 for refractive index from 1.33 to 1.43.

The tests were realized at constant temperature at 24℃, in order to avoid an influence over the liquids. Each container of automotive liquid was kept closed until its interrogation process to avoid its pollution.

The following description of the automotive liquids tests is based on the performance of the eSMS3 device, where its wavelength peak reference is positioned at 793.79 nm. The experimental results of the three fabricated devices are shown in Fig. 11 and Table I. Due the refractive index of ethanol it is practically the minimum concentration stablished for automotive coolants (70/30=1.3582), it will be useful as a reference to evaluate the quality concentration in the mentioned automotive liquids.

Thanks to the experimental tests in ethanol, that have allowed to verify that the 1 and 2 coolant samples (804.61 and 805.91nm) do not accomplish the minimum concentration stablished (70/30) due its wavelength shifts are below of the obtained by the ethanol (807.96 nm). The wavelengths shift of the 3rd, 4th and 5th coolant samples (808.33, 809.26 and 811.99 nm, respectively) against the obtained by the ethanol, allow to confirm that they satisfy the minimum concentration (70/30). Even, is observable that, a slight difference between the 4th and 5th coolant samples, it is mentioned because in both cases the manufacturers stablish in their products labels a concentration of 67/33.

The 1st and 2nd antifreeze samples (812.04 and 815.75 nm), show a certain closeness with the 5th coolant liquid, meaning that, these samples cannot be considered as an antifreeze rather coolant liquids. Remembering that, the minimum required concentration in the antifreeze liquids is 5/95. Have remarkable longer wavelengths shift-the 3rd and 4th antifreeze samples 826.10 and 834.56 nm), both positioned in closeness of ethylene glycol wavelength shift (827.20 nm), meaning a high concentration of ethylene glycol. So, the 3rd and 4th antifreeze samples accomplish with the requirements to be considered antifreeze liquids.

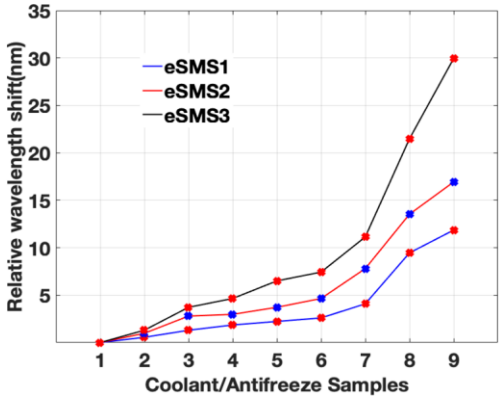

Fig. 11. Relative wavelength shifts of the devices: eSMS1, eSMS2 and eSMS3 for different coolant and antifreeze samples as a function of the refractive index of each sample.

TABLE I.

WAVELENGTH SHIFTS OF EACH SAMPLE OF COOLANT/ANTIFREEZE IN THE DEVICES: eSMS1, eSMS2 AND eSMS3.

Devices	**eSMS1**	**eSMS2**	**eSMS2**
Wavelength Peak(nm)	801.21	800.146	793.79
Samples	λ_{eSMS1} **(nm)**	λ_{eSMS1} **(nm)**	λ_{eSMS1} **(nm)**
Water	806.29	806.47	803.12
Ethanol	807.97	810.37	807.96
Ethylene glycol	818.34	826.65	827.20
Coolant 1	806.66	807.77	804.61
Coolant 2	807.03	809.74	805.91
Coolant 3	807.59	810.56	808.33
Coolant 4	807.963	810.74	809.26
Coolant 5	808.70	811.41	811.99
Antifreeze 1	809.44	812.41	812.04
Antifreeze 2	810.93	815.56	815.75
Antifreeze 3	815.38	821.30	826.10
Antifreeze 4	818.53	824.70	834.56

D. Temperature sensitivity of eSMS structures

In order to demonstrate the temperature performance in etched SMS, these have been tested in a heat surrounding medium, being this the fourth antifreeze liquid. The tests were realized in a temperature from 50 to 150°C, with increments of 10 degrees. The experiments allow to measure a nonlinear response when the temperature increases in each device: eSMS1 $\approx -.4\, nm/°C$, eSMS2$\approx -.7\, nm/°C$, eSMS3 $\approx -1.3\, nm/°C$ (see Fig. 12). It is important to note that, when the temperature increase, the RI in the external medium and sensitivity decreases. The phenomenon of nonlinearity obtained in these tests is corroborated by [16].

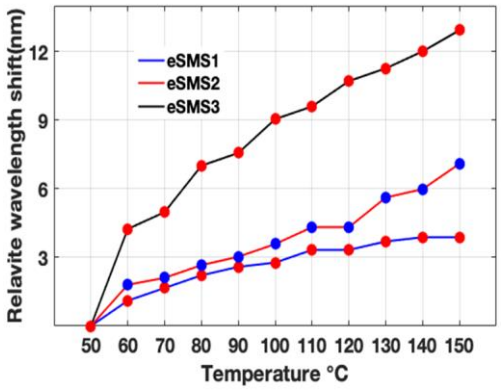

Fig. 12. Performance in a heat environmental of the eSMS1, eSMS2 and eSMS3 immersed in the antifreeze sample 4 from 50 to 150 Celsius degrees.

V. CONCLUSIONS

In this work, it has been developed a fabrication technique for tuning the diameter of SMS structures by monitoring the apparition of the self-image (fourth order and its previous order images) by means of adjusting its segment length of MMF-NC when the mentioned section of the structure is reduced by etching. Three etched SMS structures have been fabricated with different diameter using the etching process by HF. The developed devices have been monitored, verified experimentally and applied in a refractometric analysis to verify the concentration of automotive coolants and antifreeze liquids. The experiments allowed to confirm the concentration of ethylene glycol/water provided by the manufacturers in the specification charts for coolant and antifreeze liquid samples. The maximum wavelength shift was reached by eSMS3$\approx 34\,nm$, due the reduction of its diameter until a fourth part of the original (125 μm).

The presented research can be useful to fabricate etched SMS structures with diverse lengths of MMF-C according to the purposes of the applications, allowing the implementation of short or long sensitive regions. These devices could also be used for the deposition of thin films (by dip-coating or layer-by-layer) towards the obtention of biological and chemical sensors.

REFERENCES

[1]. E. Udd, W. B. Spillman Jr, "Fiber Optic Sensors: An introduction for engineers and scientists", 2nd. ed., Willey, 2011.

[2]. L.B. Soldano, E.C.M. Pennings, "Optical multi-mode interference devices based on self-imaging: principles and applications", Journal Lightwave Technology, vol. 13, no. 4, pp-615-627, 1995.

[3]. Q. Wu, Y. Semenova, P. Wang, and G. Farrell, "High sensitivity SMS fiber structure based refractometer- analysis and experiment", Optics Express, vol. 19, no. 9, pp. 7937-7944, April 2011.

[4]. A. Asseh, S. Sandgren, H. Ahlfeldt, B. Sahlgren, R. Stubbe, and G. Edwall, "Fiber Optical Bragg Grating Refractometer," Fiber Integr. Opt., vol.17, no.1, pp. 51–62 1998.

[5]. M. Myśliwiec, J. Grochowski, K. Krogulski, Krzysztof, P. Mikulic, W.J. Bock, M. Smietana. "Effect of Wet Etching of Arc-Induced Long-Period Gratings on Their Refractive Index Sensitivity". Acta Physica Polonica Series a. vol.124, no.3, pp. 521-524, 2013.

[6]. J. E. Antonio-Lopez, P. LiKamWa, J. J. Sanchez-Mondragon, D. A. May-Arrioja, "All-fiber multimode interference micro-displacement sensor", Measurement Science and Technology, vol. 24, no. 5, 7pp, April 2013.

[7]. J. G. Aguilar-Soto, J. E. Antonio-Lopez, J. J. Sanchez-Mondragon, D. A. May-Arrioja, "Fiber Optic Temperature Sensor Based on Multimode Interference Effects", Journal of Physics: Conference Series, vol. 274, no. 1, 5pp, 2011

[8]. J. Goñi, I. Del Villar. F. J. Arregui. I. Matias. Oct.-Nov. 2017. "Sensitivity enhancement by diameter reduction in low cutoff wavelength single-mode multimode single-mode (SMS) fiber sensors". Presented at 2017 IEEE Sensors. Available: https://ieeexplore.ieee.org/document/8234368

[9]. W.E. Rodríguez-Rodríguez, I. Del Villar, C.R. Zamarreño, I.R. Matias, F.J. Arregui, A.J. Rodríguez-Rodríguez, R.F. Domínguez-Cruz, "Sensitivity enhancement experimental demonstration using a low cutoff wavelength SMS modified structure coated with a pH sensitive film", Sensors and Actuators B, vol. 262, pp. 696–702, Feb. 2018.

[10]. Md. Rajibur Rahaman Khan, A.V. Watekar, and S.-W. Kang, "Fiber-Optic Biosensor to Detect pH and Glucose", IEEE Sensors Journal, vol. 18, no. 4, pp.1528-1538, 2018.

[11]. A.J. Rodríguez-Rodríguez, O. Baldovino-Pantaleón, R. F. Domínguez-Cruz, C. R. Zamarreño, I. R. Matias, D. A. May-Arrioja, "Gasohol Quality Control for Real Time Applications by Means of a Multimode Interference Fiber Sensor", Sensors, vol.14, no.19, pp. 17817-17828, 2014.

[12]. A.J. Rodríguez-Rodríguez, R.F. Dominguez-Cruz, D.A. May-Arrioja, I.Matias-Maestro, F.J. Arregui, C.Ruiz-Zamarreño, Nov.2015, "Fiber Optic Refractometer based in Multimode Interference effects (MMI) Using Indium Tin Oxide (ITO) Coating", Presented at IEEE Sensors 2015. Available: https://ieeexplore.ieee.org/document/7370600

[13]. J. E. Antonio-Lopez, I. Hernandez-Romano, D. A. May-Arrioja, J. J. Sanchez-Mondragon, Oct. 2009, "Optofluidic Tuning of MMI Bandpass Filter,". Presented at Frontiers in Optics 2009/Laser Science XXV/Fall 2009 OSA Optics & Photonics Technical Digest. Available: https://www.osapublishing.org/viewmedia.cfm?uri=FiO-2009-FTuD6&seq=0

[14]. L. Z. Jiao, D. M. Dong, W.G. Zheng, W.B. Wu, C.J. Shen, H. Yan, "Research on fiber-optic etching method for evanescent wave sensors", Optik, Vol. 124, 2013.

[15]. P. Zaca-Morán, J.P. Padilla-Martínez, J.M. Pérez-Corte, J.A. Dávila-Pintle, G.G. Ortega-Mendoza, N. Morales, "Etched optical fiber for measuring concentration and refractive index of sucrose solutions by evanescent wave", Laser Physics, Vol. 28, 2018.

[16]. S. Silva, E. G. Pachon, M. A. Franco, J. G. Hayashi, F. X. Malcata, P. Jorge, C. M. Cordeiro, "Ultrahigh-sensitivity temperature fiber sensor based on multimode interference", Applied Optics, vol. 51, 16, 2012.

[17]. A. Leung, P- Mohana Shankar, R. Mutharasan, "A review of fiber-optic biosensors", Sensors and Actuators B, Vol. 125, 2007.

[18]. Ministry of Commerce and Industrial Promotion Mexican Norm," Automotive Industry -Antifreeze / Coolant - Specifications: NMX-D-254-1987", México [Online], Available: http://www.veldoom.com/NOM/nmx-d-254-1987.pdf

[19]. J. A. Lima and G. R. Otterman, "Manual on Selection and Use of Engine Coolants and Cooling System Chemicals", Ed. 4th,

Baltimore, MD, USA, American Society for Testing and Materials (ASTM), 1989.
[20]. G. Garbincius, et al., "The influence of coolant scale deposit inside the internal combustion engine on the piston and cylinder deformations", Transport, vol 20, no. 3, pp.123-128, 2005.
[21]. Refractive Index Database [Online]. Available: https://refractiveindex.info
[22]. I. Del Villar, A. B. Socorro, J. M. Corres, F. J. Arregui, and I. R. Matias, "Refractometric sensors based on multimode interference in a thin-film coated single-mode–multimode–single-mode structure with reflection configuration", Applied Optics, vol 53, no. 18, pp.3913-3919, 2014.

Biographies

Wenceslao Eduardo Rodríguez-Rodríguez is Electronic Engineer (2011), he received the M.S. degree in Electrical and Electronic Engineering in 2013, respectively from the Autonomous University of Tamaulipas (UAT, Mexico). His research includes optical fiber sensors and embedded systems. During 2017 and 2018 did scientific visits at the Sensors Laboratory from the Public University of Navarra (UPNA), Spain.

Adolfo Josué Rodríguez-Rodríguez is Electronic Engineer (2006) and M.S. in Electronic Engineering in 2009 by the Academic Multidisciplinary Unit Reynosa-Rodhe (UAMRR-UAT). Received PhD in Communications Technologies (2014) with specialization in Fiber Optics Sensors by UPNA. Currently he manages the Computer Systems Engineer since 2015 and the Master in Computational Sciences and Technologies at UAMRR-UAT. He is coauthor of several scientific articles in embedded systems for detection of environmental parameters.

C. R. Zamarreño obtained his PhD in Communications from the UPNA in 2009, in 2012 he gained a Permanent position as Associate Professor at the UPNA and he has been working as visiting scientist at the MIT, Siemens, and UTFPR in 2008, 2011, 2013 and 2016 respectively. In 2013 he received the IEEE GOLD Award for his contributions to the development of novel optical sensing waveguides based on micro and nanostructured films where he has coauthored more than 100 scientific papers, most of them related to optical sensors based on Lossy Mode Resonances. He has also participated in 20 different research projects and is a co-founder of the spin-off company PYROISTECH SL."

Ignacio Del Villar received the M.S. degree in electrical and electronic engineering and the Ph.D. degree, specialty in optical fiber sensors, in 2002 and 2006, respectively, from the UPNA. During 2004, he was a visiting scientist with the Institute d'Optique, Orsay, France, and in 2005, he was a visiting scientist with the Applied Physics Department, University of Valencia, Spain. His research interest includes optical fiber sensors and the effect of nanostructured coatings deposited on waveguides, where he has coauthored more than 100 chapter books, journals, and conference papers. He has been a Reader with the UPNA since 2008, and an Associate Editor of the Optics & Laser Technology Journal since 2012 and of the MDPI Sensors Journal since 2017.

Manuel Zúñiga-Alanís is an Agroindustry Engineer in 1988 by the UAMRR-UAT. He is a Doctor in Education. Currently he is the Director of the UAMRR since 2015. He is co-author of several scientific articles in Mechanical Engineering applied to industrial process and instrumentation.